Journal of Materials Research and Technology 33 (2024) 1276–1285

Contents lists available at ScienceDirect

Journal of Materials Research and Technology

journal homepage: www.elsevier.com/locate/jmrt

Wire laser additively reinforced blanks: Effect of the laser power on the bending strength of a single layer reinforcement

Emanuele Fulco [a], Donato Sorgente [a,b,*]

[a] School of Engineering, Università degli Studi della Basilicata, Via Ateneo Lucano, 10, 85100, Potenza, Italy
[b] Department of Mechanics, Mathematics and Management, Politecnico di Bari, Via Orabona, 4, 70125, Bari, Italy

ARTICLE INFO

Handling editor: L Murr

Keywords:
Laser metal deposition (LMD)
Wire-laser metal deposition (w-LMD)
Al–Si coated 22MnB5 steel
316 L stainless wire
Bending test
Mechanical properties
Patchwork blanks
Tailored blanks
Wire-laser additive reinforced blanks
w-LARB

ABSTRACT

This study investigates the application of Wire Laser Metal Deposition (w-LMD), a form of Directed Energy Deposition (DED) additive manufacturing, to enhance the production process of automotive components, specifically through the development of patchwork blanks with localized reinforcements. The research focuses on reinforcing 22MnB5 steel sheets with beads of 316L steel using a laser beam at various power levels, aiming to achieve maximum strength with minimal use of material. The resulting components, referred to as wire-Laser Additively Reinforced Blanks (w-LARB), demonstrated a substantial increase in strength, up to 87%, as verified by bending tests. Notably, the study reveals that a relatively low laser power can still yield significant mechanical improvements, underlining the efficiency of the process in terms of material usage and energy consumption. Furthermore, the high repeatability of the w-LMD process confirms its potential for widespread industrial adoption in automotive manufacturing.

1. Introduction

To guarantee long-term market competitiveness and reduce CO_2 emissions, lightweight construction combined with high-performance and resource-efficient manufacturing processes is a key aspect [1–3]. Vehicle lightweighting is one of the principal requirements in the building of low-impact products such as electric vehicles (EVs), battery electric vehicles (BEVs), hybrid electric vehicles (HEVs) and plug-in hybrid electric vehicles (PHEVs). One way to maximize the energy efficiency of EVs is the reduction of the vehicle mass through lightweighting solutions for the body-in-white [4]. In a world where the transition to a low-carbon economy is a key-aspect, hybrid manufacturing processes, which combine traditional and advanced methods such as additive manufacturing, can be an effective response to the new challenges imposed by increasingly stringent regulations. This is particularly relevant in the automotive industry since the overall dimensions of cars were enlarged, and since the demands for safety and comfort has increased, the need for optimized-weight components and new manufacturing technique for the body in white of vehicles become stronger [5]. The concept of tailored blanks was proposed since 1985 [6] to meet the requirement for lightweight construction. Instead of manufacturing a full reinforced component that can lead to an increase in weight, so in fuel consumption, the concept idea was to apply the principle of reinforcing the body in white only in the areas where a higher strength or stiffness is necessary, while at the same time weight and production costs may be reduced. Tailored blanks, a key concept in the automotive field, are sheet metal components meticulously engineered to meet the specific requirements of different vehicle models, by optimizing material usage, and by minimizing material waste. Mainly, four sub-groups of tailored blanks can be found: tailor welded blanks, patchwork blanks, tailor rolled blanks and tailor heat treated blanks [7].

Patchwork blanks are based on the principle to add a flat piece of sheet metal, the patch, onto a blank in a specific area where stiffness and crash worthiness need to be improved, a process that would be challenging to achieve with a single piece of sheet metal, Fig. 1.

Advanced manufacturing techniques, such as spot laser welding or adhesive bonding, are used to seamlessly integrate individual patches. Generally, there are two strategies to apply the sheet metal patch: the first one is applying all weld spots prior to the forming process to avoid any additional welding steps after the forming, the second one is applying a few welding spots before forming, just to position the patch on the blank, and after the forming operation additional spot welds are

* Corresponding author. Department of Mechanics, Mathematics and Management, Politecnico di Bari, Via Orabona, 4, 70125, Bari, Italy.
E-mail address: donato.sorgente@poliba.it (D. Sorgente).

https://doi.org/10.1016/j.jmrt.2024.09.036
Received 2 July 2024; Received in revised form 5 September 2024; Accepted 7 September 2024
Available online 10 September 2024

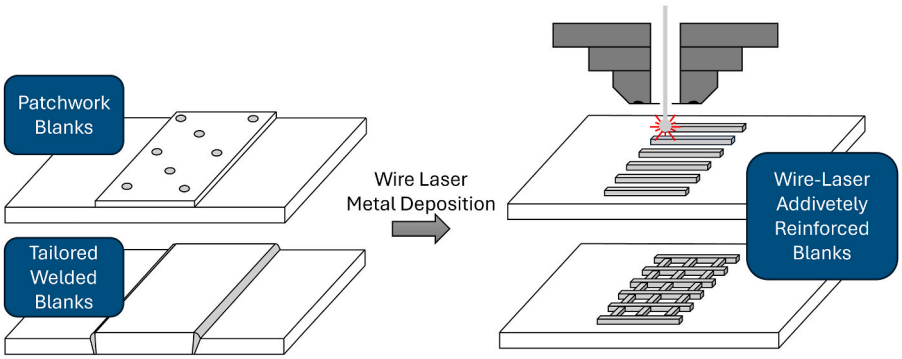

Fig. 1. Schematic representation of the different approaches. A comparison between the traditional approach and the traditional combined with additive manufacturing for reinforcement purposes; The w-LARB technology enables the fabrication of a diverse range of reinforcement geometries by reducing the amount of stiffer material required.

applied [7,8].

However, there are several disadvantages [9] in the use of patchwork blanks with the actual manufacturing processes.

- Structural discontinuities in the sheet metal which could compromise the strength and durability of the produced part;
- Susceptibility to corrosion because of the air-gaps between the sheet metal patch and the base material (due to the spot welding joints);
- Low formability for further processing.

In comparison with tailored welded blanks, patchwork blanks components allow to obtain a reduced number of cutting operations and the abolition of expensive edge preparation. However, further improvements in the use of patchwork blanks can be made.

Recent studies [10] have shown that the sheet metal has the greatest energy-environmental impact in motor vehicle production. The aim is to identify an advanced methodology that can effectively reduce the impact of patchwork production to better meet the sustainability goals of the new production requirements. A potential strategy to improve patchwork blanks is to create highly localized reinforcements by implementing Additive Manufacturing (AM): it is an advanced technology that can be useful in this context to create stiffened components which may lead to an improved version of the patchwork blanks in terms of energy-environmental impact. AM applied to the concept of patchwork blanks can allow to create highly localized reinforcements with minimal use of sheet reinforcing material – and can lead to products where all the previously mentioned disadvantages are reduced or eliminated. Some possible examples are presented in Fig. 1.

AM is an emergent technology that is widely used due to its possibility to reduce the amount of process scrap and energy consumption during the production of components. Due to its intrinsic additive property, in comparison with subtractive manufacturing processes, in which one starts with a block of material and removes away any unwanted material until one is left with the desired part, AM enables to the creation of components from nothing and builds the part one layer at a time until the part is completed with a reduction of material waste. Additionally, it has been shown that combining additive and subtractive manufacturing can lead to a reduction of material waste and manufacturing time [11].

Currently, AM processes with metals use different types of feedstocks, such as powder or wire, to create three-dimensional components by adding material layer by layer [12].

An effective method for AM is the laser metal deposition [13], LMD, a Directed Energy Deposition (DMD) technique. LMD is a process that can be industrially used either for cladding - to apply a broad range of materials (Metals such as Steel, Aluminum, Titanium, Nickel, Gold, Ceramics, Polymers) on parts, tools or substrate or for rapid prototyping/manufacturing - complex high value parts, parts repair, rebuilding of over machined areas etc. [14]. It has also been investigated for creating components with an increased strength capacity.

The use of powders is largely diffused thanks to the high laser absorption rate and the ability to produce a high surface finish [13]. However, the use of powders can be expensive due to the technological process required to obtain a powder feedstock, whereas for large geometries wire-based processes such as wire laser metal deposition (w-LMD), have significant advantages due to process speed, efficiency and high part density (very limited porosity by setting the correct printing parameters). Gao et al. [15] conducted a comparative analysis of the costs, from an economic and environmental point of view, associated with different AM technologies. Their findings indicated that the powder bed melting process exhibited a higher manufacturing cost than other methods, such as Wire Direct Energy Deposition, which is the approach that this work follows. In addition, another important advantage is that a wire feedstock does not imply wastage, it allows to get cleaner process environment without metal dust pollution [13].

A comparison of powder and wire-feed laser metal deposition methods has already shown that the wire-feed can lead to better results in terms of process efficiency [16,17].

In literature, wire-feed processes have received less attention than powder-bed or powder-feed processes. Typically, wire-feed processes have been implemented in welding application rather than in creating stiffened components.

W-LMD is a production technology that is similar to welding with a filler wire using a laser or an arc welding machine. Different teams [18–20] have experimented with this technique by retrofitting welding equipment. For instance, the microstructure of single beads of Ti–6Al–4V was investigated finding that by increasing the laser beam power and the wire-speed, changes in grain dimensions in melted zone and heat affected zone can be found [18]. In the second part of their work [19], the same authors found that dimensional measurements were good indicators of the thermal history. Larger dimensions suggest an higher input due to increased melting and a wider heat-affected zone (also with larger grain sizes as observed in Ref. [18]). Additionally, they found that single bead hardness increases with the amount of base material melted.

Gruger et al. [21] investigated several different engineering tests, including bending tests, to evaluate the mechanical strength of test specimens that were fabricated by conventional manufacturing (machining), Laser Powder Bed Fusion (L-PBF) and Wire Arc Directed Energy Deposition (WA-DED), an AM technique based on a wire feedstock employing a heat source based on electric arc (WAAM). They found that the elastic load capacity of wire additively made specimens was comparable to that of the conventional ones and that the mechanical properties depend significantly on the manufacturing process.

Ge et al. [22] explored the multiple challenges in the hybridization of traditional sheet metal forming processes with the use of AM. In

Table 1
Chemical compositions of substrate material and its Al–Si coating.

[Weight %]	C	Mn	Si	S	P	Ni	Cr	Ti	Al	B	Mo	Fe
22MnB5 base material	0.22	1.28	0.23	0.01	0.01	–	0.23	0.06	0.31	0.005 max	0.01	Bal.
Al–Si coating	–	–	11.12	–	–	–	–	–	87.73	–	–	1.14

particular, they analyzed the AM-Deep drawing, AM-Flanging, AM-Spinning and AM-Incremental forming from a technical and an economic point of view concluding that, according to the production volume [23], the shape complexity and process optimizations, the hybridization could lead to a reduction of the overall costs of the production chain.

The present work explores the combination of the innovative wire AM process (w-LMD) with the concept of sheet patchworks. In particular, AM is not employed for wear protection or repairing purposes [24], but with the aim of strengthening an existing blank, exploiting the high material deposition efficiency [13]. The aim of this study is to investigate the feasibility of integrating AM into the manufacturing process of patchwork blanks to apply reinforcements to an existing sheet metal substrate. The previously aforementioned limits of the traditional patchwork blanks could be effectively addressed through the integration of AM technology, thus providing a comprehensive solution that offers the advantages of both traditional and innovative manufacturing techniques. In literature, there have been only a few studies about AM process hybridization, most of them related on microstructure analysis, but, to the best of our knowledge, none of them related to the strength characterization of reinforcements obtained by w-LMD. In this work, bending tests are carried out to assess the effect of additive process parameters on the flexural mechanical behaviour of reinforced blanks. In this context, the concept of wire-Laser Additively Reinforced Blanks, w-LARB, is presented.

Furthermore, this novel hybrid process allows for the investigation of a multitude of potential combinations of reinforcement material and substrate, provided that they are capable of being welded together. Also, this approach could eventually lead to reduce material waste related to the manufacturing process.

2. Materials and methods

2.1. Materials

The experimental campaign was carried out on 22MnB5 boron steel sheets with a 1.5 mm nominal thickness. This type of steel is widely used in the automotive industry due to its excellent combination of mechanical strength and formability. Low boron additions to the composition provide high hardenability and improved mechanical properties making it suitable for applications that require high-strength and lightweight parts, resulting in up 50 % savings in weight compared to conventional steel. 22MnB5 steel is commonly used in the hot stamping process [25].

During the preparation step, the substrate was prepared by applying an Al–Si coating. This metallic coating is generated in a continuous hot-dip galvanizing process [26] in which the base material, that has been cleaned to remove any residual trace of oxide, is immersed in a molten pool of aluminum and silicon at elevated temperatures, forming a protective coating of Al–Si. This is necessary to prevent oxide scale formation and decarburization on the surface of the austenitized sheet metal during the hot stamping process [27].

Table 1 provides the chemical composition of the stainless steel and its coating [27,28].

The deposited material was 316 L stainless steel, which is a versatile and widely used material known for its excellent corrosion resistance, high strength and durability. These properties make it suitable for applications in modern industries such as chemical production, nuclear production, aerospace, train and ship manufacture [29]. The use of 316L stainless steel as reinforcement can be expected to result in enhanced durability and reliability for the stiffened component.

Table 2
Chemical composition of 316 L stainless steel wire.

[Weight %]	C	Mn	Si	Ni	Cr	Mo	Fe
316 L Wire-added material	0.02	1.7	0.9	12.0	18.5	2.7	Bal.

It belongs to the austenitic stainless-steel family with chromium-nickel. The 316 L wire had a diameter of 1.0 mm. Its chemical composition is given in Table 2 [30].

22MnB5 steel offers high mechanical strength, while 316L steel provides good corrosion resistance. By using a combination of both, it can be possible to optimize the overall performance of the patchwork blank, providing both good mechanical strength and corrosion protection.

2.2. Reinforcement deposition by AM

Fig. 2a depicts the experimental equipment, which includes a Meltio M450 3D-wire printing machine capable of producing high-density metal parts in a single-step process. The print envelope dimensions (W x D x H) are 145 x 168 × 390 mm. The 316 L wire is front fed at an angle of 90° to the horizontal. Additionally, an inert gas nozzle (Argon, 99 % purity) is co-axially positioned with the wire to protect the working area against oxidation.

The power source consists of 6 × 200 W direct diode lasers with a wavelength of 976 nm, providing a total laser power of 1200 W under the maximum working conditions. Fig. 2b) offers a schematization of the laser head. To facilitate the deposition, the hot wire technique was used during the printing process, an option that increases the printing speed of the system by pre-heating the wire through the Joule effect before it is melted by the six laser beams and enters in the melt pool. Hot wire works by creating an electric current from the deposition head through the unmolten wire to the build-plate which is grounded. The stainless steel has the highest electrical resistance in the hot wire circuit, so it heats up preferentially. The value of the electric current used for hot wire was 2 A.

The printing machine is also equipped with a 5 kW active water-cooler chiller set at 16.0 °C, and an air filtering system.

The dimensions of the substrate material blanks, (W x H) 125 × 200 mm, were established according to the dimensions of the machine's workpiece table, (W x H) 150 x 200 mm. The thickness of the substrates was of 1.52 ± 0.004 mm. A sheet clamping system was built using two drilled brackets positioned on the shortest sides of the substrate plates, as shown in Fig. 3. The two brackets were necessary to clamp the plate onto table below to prevent small displacements caused by the inertia during of the table movements.

A single-factor experimental plan was developed in order to obtain different deposition power configurations for each metal sheet plate. A straight-line deposition geometry was considered for reinforced specimens, oriented in the same direction of the longest side of the specimen in order to match the direction of the neutral line during the bending test. The blanks were cut with the rolling direction parallel to the longest side (200 mm), resulting in the reinforcement being deposited in the same direction.

Six equally spaced reinforcements were deposited on each substrate

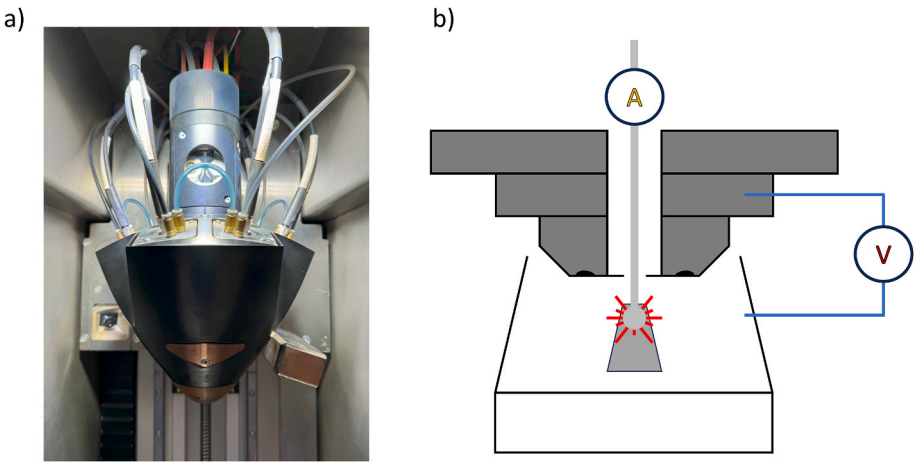

Fig. 2. a) Wire laser additive manufacturing laser head; b) schematization of the laser head and the printing process.

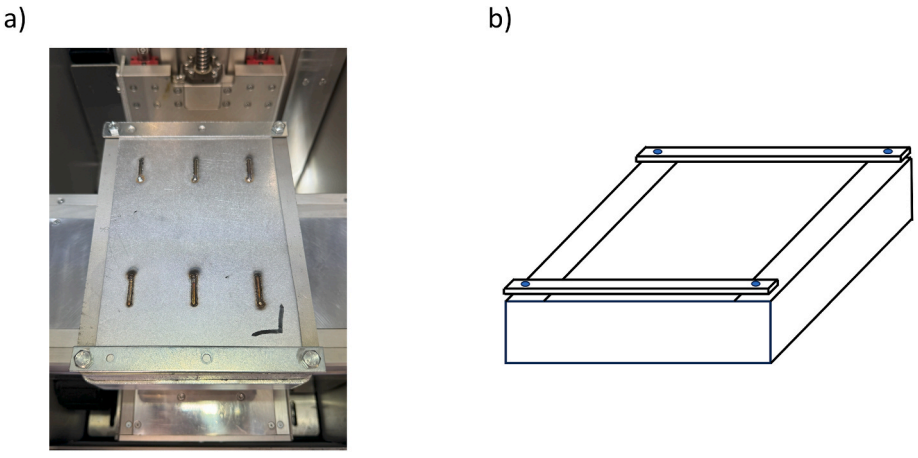

Fig. 3. a) Sheet clamping system; b) schematization of the two brackets of the clamping system necessary to maintain the sheet in a fixed position on the working table.

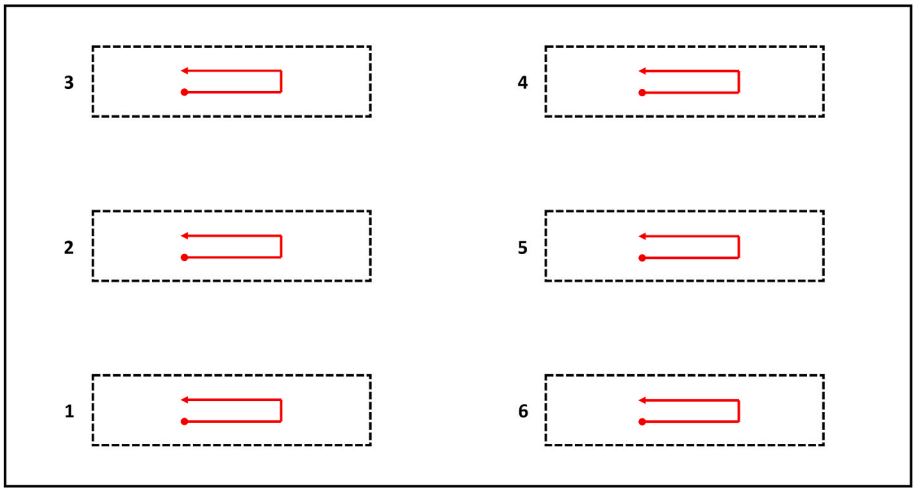

Fig. 4. A schematic representation of the six equally-spaced specimens onto the 22MnB5 base sheet material.

plate using different power deposition values. The nominal dimensions of the reinforcements set in the toolpath generator software (Horizon, Meltio) were 20 mm in length, 2 mm in width (two passes) and 1 mm thick.

In the experimental plan, only one layer was deposited to observe improvements under this simple condition, and also to minimize thermal distortions. The power range considered was between 700 W and 1200 W, in increments of 100 W. On a single plate, two replications of the same power can be found. In Fig. 4 a schematic representation of the printing geometry is presented. The beads were printed in a clockwise

Table 3
Specifications of laser welding system.

Laser Power [W]	Printing Speed [mm/min]	Deposition feed rate [mm/min]	Inert gas flow (Argon) [l/min]
700 ÷ 1200	450	450	10

order from the first to the sixth and final reinforce to control the thermal load and avoid substrate distortions.

The printing parameters are listed in Table 3.

After the additive deposition of the 316 L stainless steel, sections were performed on the sheet metal plate in order to obtain the bending specimens.

2.3. Bending tests

Bending specimens were rectangular with the following dimensions: 80 ± 0.5 mm in length, 20 ± 0.4 mm in width, as shown in Fig. 5, and the same thickness of the substrates.

The three-point bending tests were conducted using an Instron 5982 universal testing machine, as shown in Fig. 6. Flat specimens, with previously reported dimensions, were used according to EN ISO 7438:2020 [31].

Specimens were extracted by a metallographic cut-off machine from the blanks and on each single specimen the reinforcing bead was measured to evaluate its effective dimensions.

The punch had a diameter D of 10 mm and its travel speed was set to 2 mm/min. A maximum stroke of 12 mm was used for all specimens. The lower anvils were placed in order to have a span, *l*, of 40 mm. In all the tests, the reinforcement was placed on the opposite side of the punch, i.e. below. Furthermore, the specimen was centered between the anvils with reference to the length of the reinforcement. The outputs of the bending test were the force measured by the load cell of the machine, *F*, the flexural stiffness, *K* and the modulus of elasticity, *E*. The first quantity is directly acquired by the load cell signal with a frequency of 10 Hz. Flexural stiffness and modulus of elasticity were calculated as follows:

- Flexural Stiffness, *K*: it expresses the resistance that an element opposes to the deformation imposed by bending. It is a function of the Young's modulus, *E*, the second moment of area, *I*, and the flexural displacement of the beam, *δ*. It is calculated as the ratio between force and displacement in the elastic section of the force-displacement curve, so as a direct consequence of force and displacement measured during the test;

$$K = \frac{F}{\delta} \tag{1}$$

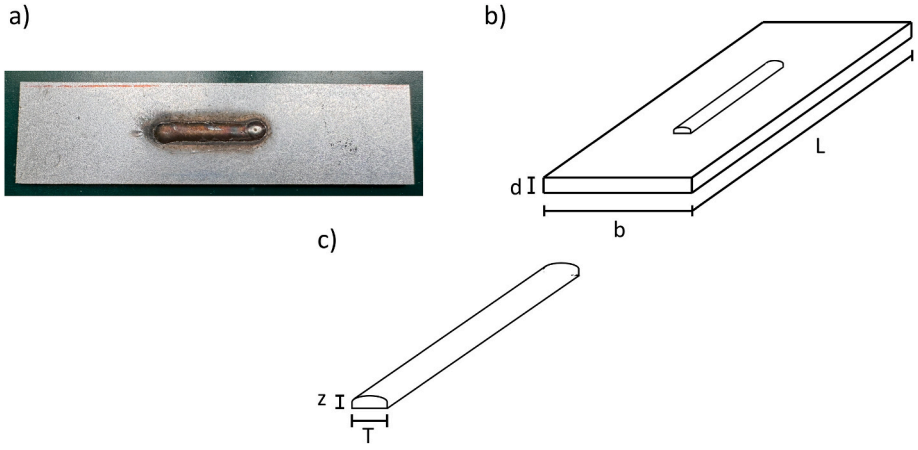

Fig. 5. a) Reinforced specimen before bending; b) reinforced specimen schematization with nominal dimensions of b = 20 mm, L = 80 mm, and d = 1.5 mm; c) dimensions of the elliptic-reinforce: T major axis, z minor semi-axis.

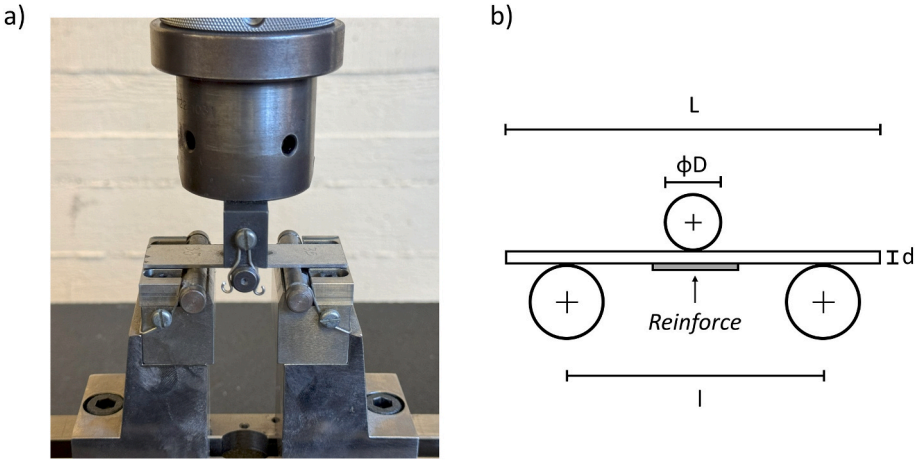

Fig. 6. a) Three-point bending tools; b) schematization of the bending set-up in which the reinforce has been positioned on the opposite side of the punch and centered between the anvils.

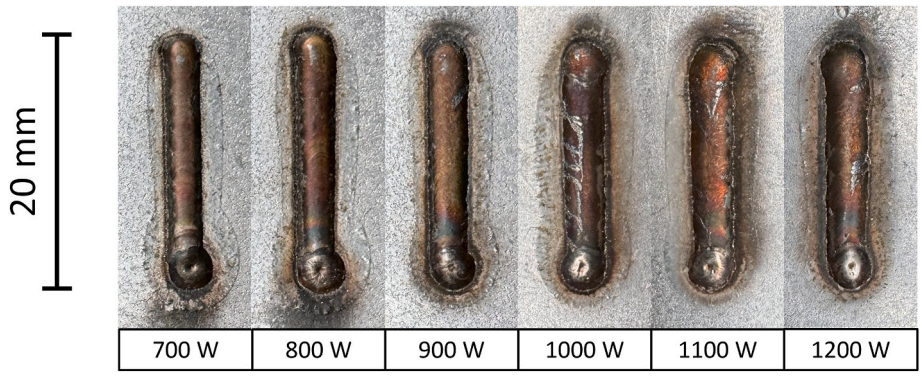

Fig. 7. Front view of the morphology of 316 L bead reinforcements.

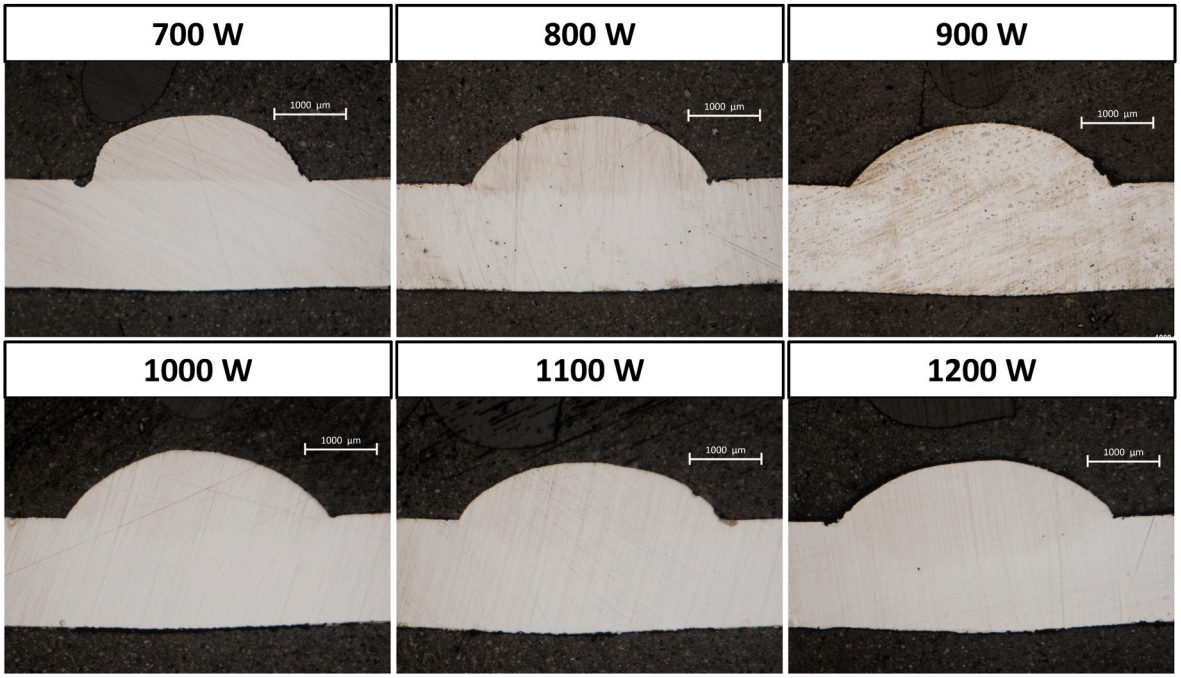

Fig. 8. Section view of the morphology of the 316 L bead reinforcements.

- Modulus of Elasticity: for a multi-material section, which is defined as a combination of two or more different materials, the modulus of elasticity E has to be considered as an equivalent modulus, E_{eq}. It can be determined starting from the Flexural Stiffness. From a mathematical point of view, according to the Euler-Bernoulli beam theory, the flexural displacement of the beam can be evaluated by the double integration of the moment-curvature equation:

$$M = -EI\frac{d^2\delta}{dx^2} \tag{2}$$

where x is the distance along the beam.

For a three-point bending test, the deflection of a beam with a centered load can be expressed as follows:

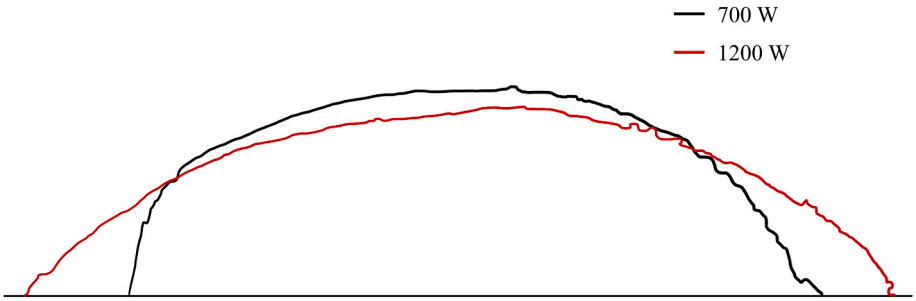

Fig. 9. A comparison of the cross-sectional view between a specimen reinforced at 700 W and one reinforced at 1200 W. When increasing the laser power, an increase in the reinforce width can be seen.

Table 4
Major and minor dimensions, aspect ratio of the reinforcements for different power values.

Power [W]	T [mm]	z [mm]	Aspect Ratio z/T
700	3.065	0.954	0.3112
800	3.240	0.966	0.2981
900	3.633	0.900	0.2478
1000	3.538	0.928	0.2624
1100	3.657	0.865	0.2364
1200	3.848	0.854	0.2219

$$\delta = \frac{FL^3}{48E_{eq}I} \tag{3}$$

So, the equivalent elastic modulus can be written in the following form:

$$E_{eq} = \frac{KL^3}{48I} \tag{4}$$

Where the ratio F/δ has been written as K.

3. Results and discussion

3.1. Macroscopic morphology of the deposited beads

Fig. 7 shows the morphology of the reinforced 316L beads by varying the power source from 700 W to 1200 W.

Figs. 7 and 8 show how the top view and the cross-section of the reinforcing beads change in function of the deposition power. Higher power results in wider beads, while lower power results in narrower and thicker beads. Fig. 9 presents a comparison of the different profiles (obtained by analysis of the images of the cross sections) of the reinforcements made with 700 W and 1200 W.

This different behaviour can be attributed to the different heat input in each power case. When depositing at higher powers, the temperature difference between the material and its surroundings is greater than the one that obtained when depositing at lower powers. Because of the highest peak temperature [32], both surface tension and viscosity decrease resulting in wider and thinner reinforcement beads. Cooling occurs more rapidly for reinforcements deposited with less power, so as the surface tension will be higher, beads will be thicker. Xu et al. [13] found a similar effect, where a higher heat input resulted in a lower aspect ratio for the bead.

Reinforcements were measured by optical microscopy to identify quantitative dimensional differences between the different laser power inputs. The average dimensions and the aspect ratio measured for each power level are listed in Table 4.

T and z dimensions, respectively, represent the major axes and the minor semi-axis of an ellipse that was used to approximate the irregular section-shape of the reinforcing material, Fig. 5 c). Also, the cross section-view in Fig. 8 can be explicative about the results provided in Table 4.

In the experimental plan, three other configurations below 700 W (400-500-600 W) were tested to further decrease the energy demand of the process. However, these configurations are not reported due to poor quality of the reinforcement, which resulted in dripping of wire and, as a consequence, discontinuous deposition. At 400 W, the adhesion of the reinforcement to the substrate material was only partial and could cause the detachment of the reinforcement when a load is applied.

The average dimensions of the beads were used to calculate the moments of inertia of the reinforced sections in order to evaluate the modulus of elasticity of the reinforced specimens.

In addition, the moments of inertia calculated using this method were compared to the nominal moment of inertia of the section, which was determined by the bead dimensions selected during the design stage and adopted into the slicing software. The results are listed in Table 5.

Table 5
Moment of Inertia values at different power levels; comparison with the nominal moment of inertia evaluated with the nominal geometry.

Power [W]	Effective Moment of Inertia [mm^4]	Deviation (Effective vs Nominal)
700	8.609	0.046 %
800	8.930	3.777 %
900	8.695	1.046 %
1000	8.992	4.497 %
1100	8.274	−3.847 %
1200	8.597	−0.093 %

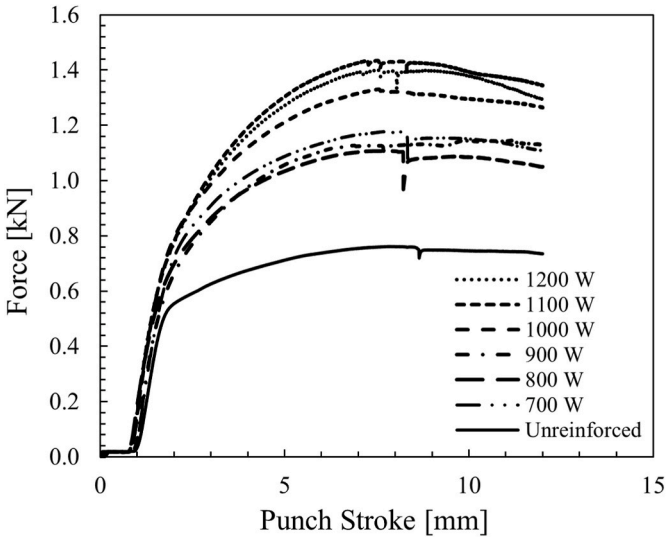

Fig. 10. Force-displacement diagram for all powers of reinforcement and a specimen in as-received conditions (Unreinforced).

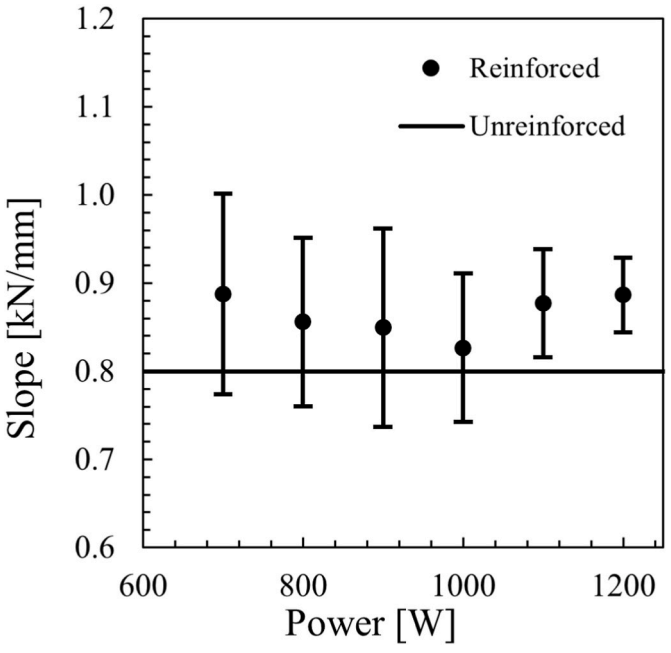

Fig. 11. Comparison of the slope of the elastic region between different power of deposition and the average value for not reinforced specimens.

For the lowest levels of the deposition power, the discrepancy between the nominal and the effective value of the moment of inertia is negligible. For the calculation of the quantities of interest in the

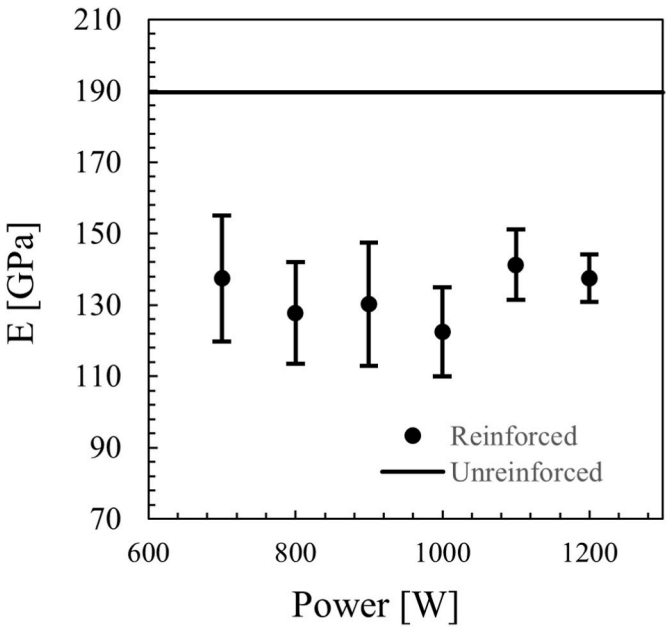

Fig. 12. Modulus of Elasticity by varying the reinforcement power.

following section of this work, the effective moment of inertia will be used as it is more representative of the specimen tested in bending, particularly those corresponding to a laser power between 1000 and 1200 W.

3.2. Bending test results

Bending tests were carried out according to the parameters shown in section 2.3. The results of each test were presented in the form of a force-displacement diagram, which was useful for comparing the different strengths of specimens when they were reinforced with different power values. As illustrated in Fig. 10, an elastic first section is clearly evident, as well as a plastic one.

The curves show a comparable behaviour in the elastic range between different reinforced blanks achieved at different laser powers. An increase in the elastic load capacity can be seen when reinforced specimens are compared with unreinforced ones.

The slope of the elastic region obtained while varying the laser power were found to fluctuate with no observable trend, as shown in Fig. 11. To confirm this, an Analysis of Variance (ANOVA) was conducted first between reinforced specimens and then between reinforced and unreinforced ones. The results suggested that the variation in power did not have a significant effect on the observed slope of the elastic behavior of reinforced specimens, with 95 % confidence. However, reinforcing the specimen had a significant effect on the slope, if the comparison is done with unreinforced specimens.

Regarding the modulus of elasticity, E, which depends on both the bending stiffness, K, and the moment of inertia of the section, I, different values of E are expected depending on the moment of inertia, which varies with the geometry of the section and the reinforcing power used.

According to Fig. 12, it is not possible to identify a clear trend in the equivalent modulus of elasticity, E_{eq}, when the laser power is varied. Nevertheless, the difference between power levels is statistically significant at a 95% confidence level, both when considering differences only within reinforced specimens and when comparing reinforced with unreinforced ones.

The E_{eq} values obtained for the reinforced specimens were lower than the typical modulus of elasticity value for the two adopted steels, which is 197 GPa for 22MnB5 [33] and 193 GPa for AISI 316 L [34]. This result can be explained by considering that the two different steels (substrate and additional reinforcing layer) are characterized by their own stiffness. Consequently, the combined displacement of the system for a given force is greater than that of any single material, resulting in a reduced overall stiffness. In fact, the equivalent moduli of elasticity of the reinforced specimens are lower than the modulus of the single material.

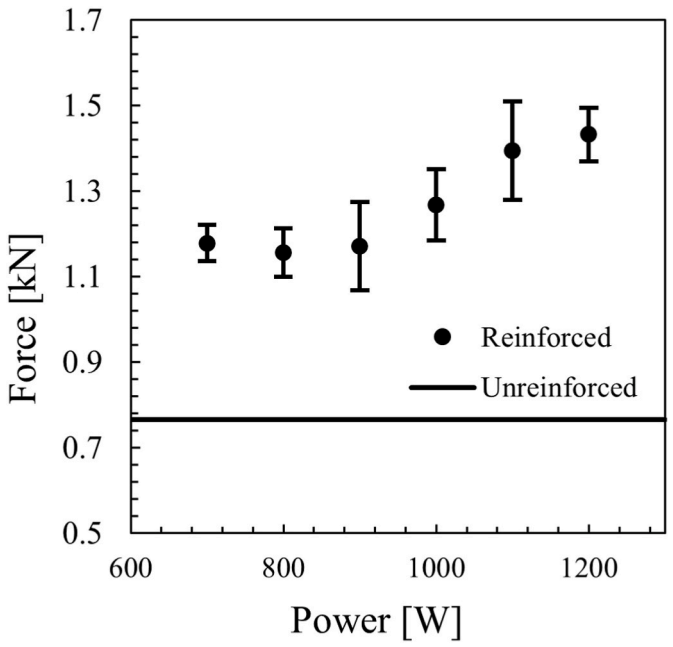

Fig. 13. Maximum force values over different conditions of reinforcement power deposition and a non-reinforced specimen.

Table 6
Force between reinforced and non-reinforced specimens.

Laser Power [W]	Force increase
700	54.08 %
800	51.22 %
900	53.14 %
1000	65.75 %
1100	82.21 %
1200	87.19 %

Fig. 13, provide an overview of the results in terms of maximum force achieved in the bending tests for different laser power values. For a better understanding of the strength enhancement, Table 6 presents a summary of the increase in load resistance of reinforced specimens in comparison to the not reinforced ones.

The mass increment was calculated by evaluating the length of wire extruded through the nozzle of the AM machine. For each reinforcement, 0.303 g of wire was required, which is the 1.6 % of the starting mass of the substrate, 18.96 g. Reinforced specimens can withstand significantly more force than the not-reinforced ones, with an increase ranging from 51 % (800 W) to 87.19 % (1200 W), a considerable increase given that the mass increment does not exceed the 2 %. Therefore, it can be concluded that, with the use of w-LMD, the goal of producing excellent performance reinforcements by adding small amounts of reinforcing material can be successfully achieved.

When specimens with similar reinforcement power are compared, no relevant differences can be seen. However, when specimens of 1200 W are compared with those of 1000 W and 700 W, an increase of 12.93 % and 21.49 % respectively can be observed.

Starting from the analysis of the moment of inertia of different specimen sections, a higher force value should be expected when decreasing power. When a beam is subjected to a given applied force, the bending resistance will be greater for elements with a higher moment of

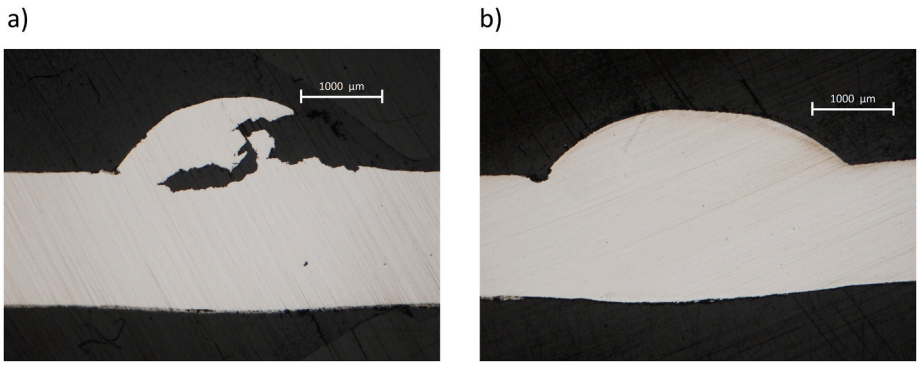

Fig. 14. After bending cross-section for a) 700 W and b) 1200 W reinforcements.

inertia. The experimental results of this study indicate that specimens reinforced with a high value of power exhibit the highest values of force. This can appear in contrast with the previous observation that specimens with higher moment of inertia also exhibit the highest values of force. To identify the underlying causes of this behavior, reinforced specimens were sectioned after bending. Fig. 14 shows the after bending cross-section view for the lowest, 14 a), and highest, 14 b), power of deposition.

Fig. 14 a) demonstrates that the 700 W reinforcement exhibits a significantly reduced resistant section. It appears to be strongly damaged and, although the moment of inertia was greater, the reduced resistant section resulted in the specimen failing more easily under lower force values than those found for the 1200 W specimen. In contrast, in Fig. 14 b), the cross section of the 1200 W specimen appears to be perfectly intact after bending.

The ANOVA revealed that the results obtained from the bending tests in terms of bending force, differed significantly from each other at a 99 % confidence level. The p-value obtained was of the order of 10^{-19}, indicating a high level of significance. These differences remained significant even when comparing only the reinforced specimens at different deposition powers, this time with a p-value of the order of 10^{-9}.

The ANOVA was also conducted to verify the repeatability of the process by comparing the results of specimens reinforced with the same power. The results suggested that the different strength values found within each power class were not statistically significant, demonstrating that the process is repeatable with a 99 % confidence interval.

In their investigation about the use of LMD with a powder feedstock to reinforce metal sheet, Ünsal et al. [24] attempted to bend reinforced specimens with an angle of 180°. No macroscopic cracks were observed on the outer surface of the specimens. This conclusion was corroborated by microscopic analysis.

In the current work, the bending angle was of 117° which corresponds to a deflection of 12 mm, as previously stated in section 2.3. With this bending angle and the w-LMD technology, there were no failures or cracks from a macroscopic point of view, with the exception of one specimen reinforced with a power of 700 W where the resistant section was completely damaged after bending. This result suggests that reinforcing at lower laser powers may provide an energy benefit and a higher moment of inertia, but does not guarantee sufficient load carrying capacity of the reinforcement.

Further investigations will include other possible solutions to revive the potential for manufacturing patchwork blanks through the application of an innovative technology, such as AM with a metal wire. It would be beneficial to investigate new reinforcement geometries that aim to increase the strength of components with custom-formed beads while minimizing the amount of added mass.

Furthermore, future work will be required to verify the performance of reinforcement following a stamping process, as well as to verify the feasibility of reinforcement applied to an already formed sheet metal substrate.

Future works will also include the production of multi-layer reinforcements, with an investigation about thermal distortions, the microstructure at the interface between the base steel and the steel added by w-LMD, as well as new material combinations. As an example, a 22MnB5 steel that has already been hardened could be considered as a substrate for future experimental works.

4. Conclusions

The following conclusions can be drawn according to the results of the experimental work reported in this work.

- W-LMD technology allowed to produce stronger components than the base material by adding just the 1.6 % of mass: from an increase in load of 54.08 % at 700 W, to an increase of 87.19 % at 1200 W;
- The equivalent moduli of elasticity of the reinforced specimens were lower than the modulus of the single material due to the combination of two different steels;
- A significant increase in the elastic load capacity and in the slope of the elastic region can be seen when reinforced specimens are compared with unreinforced ones;
- Higher deposition laser power results in wider beads, while lower values results in narrower and thicker beads;
- Lower reinforcement powers result in a notable decline in the quality of the reinforcement during bending: at 700 W a highly damaged cross section was observed with a significant reduction of resistance; at 1200 W, the reinforcement section appeared to be in good condition;
- The process was found to be repeatable with a 99 % repeatability rate when using the same deposition power, a promising result for the application of this innovative AM technology in the industrial manufacturing process of patchwork blanks.

Declaration of competing interest

The authors declare that they have no known competing financial interests or personal relationships that could have appeared to influence the work reported in this paper.

Acknowledgments

The authors would like to acknowledge the cooperation and support of the Baosteel Tailored Blanks S.r.l and of Regione Basilicata who has funded the In-LINK-IT project (PO FESR Basilicata 2014–2020, G29J19001180003). This work was partly supported by the Italian Ministry of University and Research under the Programme “Department of Excellence” Legge 232/2016 (Grant No. CUP - D93C23000100001).

References

[1] Fetting C. The European green deal. ESDN Report. Eur Comm 2020;53:24.
[2] CO_2 emission standards for new passenger cars and vans in the European Union. 2023. https://theicct.org/publication/eu-co2-standards-cars-vans-may23; [accessed 14 June 2024].
[3] Çınar G. THE green deal and the automotive industry in the eu transforming the automotive industry-impact on eu regions nd.
[4] Cimprich A, Sadayappan K, Young SB. Lightweighting electric vehicles: scoping review of life cycle assessments. J Clean Prod 2023;433:139692.
[5] Cischino E, Di Paolo F, Mangino E, Pullini D, Elizetxea C, Maestro C, et al. An advanced technological lightweighted solution for a body in white. Transp Res Procedia 2016;14:1021–30. https://doi.org/10.1016/j.trpro.2016.05.082.
[6] Kusuda H, Takasago T, Natsumi F. Formability of tailored blanks. J Mater Process Technol 1997;71:134–40. https://doi.org/10.1016/S0924-0136(97)00159-3.
[7] Lamprecht K, Geiger M. Characterisation of the forming behaviour of patchwork blanks. Steel Res Int 2005;76:910–5. https://doi.org/10.1002/srin.200506115.
[8] Lamprecht K, Merklein M, Geiger M. Hydroforming of patchwork blanks - numerical modeling and experimental validation. AIP Conf Proc 2005;778(A): 526–31. https://doi.org/10.1063/1.2011274.
[9] Bambach M, Sviridov A, Weisheit A. Stiffness management of sheet metal parts using laser metal deposition. AIP Conf Proc 2017;1896. https://doi.org/10.1063/1.5008094.
[10] Horton PM, Allwood JM. Yield improvement opportunities for manufacturing automotive sheet metal components. J Mater Process Technol 2017;249:78–88. https://doi.org/10.1016/j.jmatprotec.2017.05.037.
[11] Sathish K, Kumar SS, Magal RT, Selvaraj V, Narasimharaj V, Karthikeyan R, et al. A comparative study on subtractive manufacturing and additive manufacturing. Adv Mater Sci Eng 2022;2022. https://doi.org/10.1155/2022/6892641.
[12] Bambach MD, Bambach M, Sviridov A, Weiss S. New process chains involving additive manufacturing and metal forming - a chance for saving energy? Procedia Eng 2017;207:1176–81. https://doi.org/10.1016/j.proeng.2017.10.1049.
[13] Xu X, Mi G, Luo Y, Jiang P, Shao X, Wang C. Morphologies, microstructures, and mechanical properties of samples produced using laser metal deposition with 316 L stainless steel wire. Opt Lasers Eng 2017;94:1–11. https://doi.org/10.1016/j.optlaseng.2017.02.008.
[14] Kaierle S, Barroi A, Noelke C, Hermsdorf J, Overmeyer L, Haferkamp H. Review on laser deposition welding: from micro to macro. Phys Procedia 2012;39:336–45. https://doi.org/10.1016/j.phpro.2012.10.046.
[15] Gao C, Wolff S, Wang S. Eco-friendly additive manufacturing of metals: energy efficiency and life cycle analysis. J Manuf Syst 2021;60:459–72. https://doi.org/10.1016/j.jmsy.2021.06.011.
[16] Li F, Gao Z, Li L, Chen Y. Optics & Laser Technology Microstructural study of MMC layers produced by combining wire and coaxial WC powder feeding in laser direct metal deposition. Opt Laser Technol 2016;77:134–43. https://doi.org/10.1016/j.optlastec.2015.09.018.
[17] Heigel JC, Gouge MF, Michaleris P, Palmer TA. Journal of Materials Processing Technology Selection of powder or wire feedstock material for the laser cladding of Inconel ®625. J Mater Process Tech 2016;231:357–65. https://doi.org/10.1016/j.jmatprotec.2016.01.004.
[18] Brandl E, Michailov V, Viehweger B, Leyens C. Deposition of Ti-6Al-4V using laser and wire, part I: microstructural properties of single beads. Surf Coatings Technol 2011;206:1120–9. https://doi.org/10.1016/j.surfcoat.2011.07.095.
[19] Brandl E, Michailov V, Viehweger B, Leyens C. Deposition of Ti-6Al-4V using laser and wire, part II: hardness and dimensions of single beads. Surf Coatings Technol 2011;206:1130–41. https://doi.org/10.1016/j.surfcoat.2011.07.094.
[20] Wen P, Cai Z, Feng Z, Wang G. Microstructure and mechanical properties of hot wire laser clad layers for repairing precipitation hardening martensitic stainless steel. Opt Laser Technol 2015;75:207–13. https://doi.org/10.1016/j.optlastec.2015.07.014.
[21] Grüger L, Sydow B, Woll R, Buhl J. Design of a cost-effective and statistically validated test specification with selected machine elements to evaluate the influence of the manufacturing process with a focus on additive manufacturing. Metals 2023;13. https://doi.org/10.3390/met13111900.
[22] Ge T, Li Y, Gao D, Yang C, Li F. Hybridizing additive manufacturing and sheet forming process to manufacture complex components with multi-features: a review. J Manuf Process 2024;124:345–64. https://doi.org/10.1016/j.jmapro.2024.06.032.
[23] Gonçalves A, Ferreira B, Leite M, Ribeiro I. Environmental and economic sustainability impacts of metal additive manufacturing: a study in the industrial machinery and aeronautical sectors. Sustain Prod Consum 2023;42:292–308. https://doi.org/10.1016/j.spc.2023.10.004.
[24] Ünsal I, Hama-Saleh R, Sviridov A, Bambach M, Weisheit A, Schleifenbaum JH. Mechanical properties of sheet metal components with local reinforcement produced by additive manufacturing. AIP Conf Proc 2018;1960. https://doi.org/10.1063/1.5035054.
[25] Gracia-Escosa E, García I, Damborenea JJD, Conde A. Friction and wear behaviour of tool steels sliding against 22MnB5 steel. J Mater Res Technol 2017;6:241–50. https://doi.org/10.1016/j.jmrt.2017.04.002.
[26] Karbasian H, Tekkaya AE. A review on hot stamping. J Mater Process Technol 2010;210:2103–18. https://doi.org/10.1016/j.jmatprotec.2010.07.019.
[27] Coviello D, von der Heydt J, Rullo L, Keßler M, De Vito M, D'Angola A, et al. Laser welding of tailored blanks made of Al-Si-coated 22MnB5 steel using a filler wire and a variable energy distribution laser optics. Int J Adv Manuf Technol 2023;125: 2691–704. https://doi.org/10.1007/s00170-023-10921-4.
[28] Kolaříková M, Chotěborský R, Hromasová M, Linda M. The characteristics of al-si coating on steel 22mnb5 depending on the heat treatment. Acta Polytech 2019;59: 352–8. https://doi.org/10.14311/AP.2019.59.0352.
[29] Song RB, Xiang JY, Hou DP. Characteristics of mechanical properties and microstructure for 316L austenitic stainless steel. J Iron Steel Res Int 2011;18: 53–9. https://doi.org/10.1016/S1006-706X(11)60117-9.
[30] Meltio Materials, Stainless steel 316L datasheet. 2024. https://meltio3d.com/materials [accessed 18 September 2024].
[31] BSI. BS EN ISO 7438 : 2020 BSI Standards Publication metallic materials — bend test. 2020. p. 1–13.
[32] Leão Ferreira I, Adilson de Castro J, Garcia A. Dependence of surface tension and viscosity on temperature in Multicomponent alloys. Wettability Interfacial Phenom - Implic Mater Process 2019. https://doi.org/10.5772/intechopen.82307.
[33] Neumayer FF, Vogt S, Gueffroy M, Jesner G, Kelsch R, Geile M, et al. Warm and cold blanking of manganese-boron steel 22MnB5 with different tool geometries. Procedia Manuf 2019;29:345–52. https://doi.org/10.1016/j.promfg.2019.02.147.
[34] Yan L, Lim JL, Lee JW, Tia CSH, O'Neill GK, Chong DYR. Finite element analysis of bone and implant stresses for customized 3D-printed orthopaedic implants in fracture fixation. Med Biol Eng Comput 2020;58:921–31. https://doi.org/10.1007/s11517-019-02104-9.